J. Fluid Mech. (1967), *vol.* 27, *part* 2, *pp.* 209–230
Printed in Great Britain

Irrotational fluctuations near a turbulent boundary layer

By P. BRADSHAW
Aerodynamics Division, National Physical Laboratory

(Received 12 January 1966)

A verification of some of the predictions of the theory of Phillips (1955) is presented, and the relation between one-dimensional and two-dimensional wave-number spectra is discussed. The convection velocity of the irrotational field deduced from measurements of the frequency spectrum alone appears to be about $0{\cdot}9U_1$ in the frequency range carrying most of the energy. It follows that the pressure-fluctuation spectrum is proportional to the velocity-fluctuation spectrum and varies as ω^2 at low frequency. The discrepancy between this result and measurements of wall-pressure spectra is plausibly attributed to extraneous sound.

1. Introduction

Turbulent flows always include fluctuations of static pressure as well as vorticity. The pressure fluctuations extend beyond the rotational region into the so-called 'near field', where they are related to the velocity fluctuations by Bernoulli's equation. From another point of view, the near-field velocity fluctuations can be regarded as directly induced by the vortex lines in the rotational flow. The near-field fluctuations, being irrotational, can be described by a potential, so that they are completely specified in a given volume of space if the boundary conditions are specified: in particular they are specified in the half-space $x_2 > 0$ by the normal velocity component or 'upwash' $\partial\phi/\partial x_2$ in the plane $x_2 = 0$ and the condition $\operatorname{grad}\phi = 0$ at infinity. Phillips (1955) has obtained a very complete description of the motion corresponding to a statistically stationary (homogeneous) random distribution of $\partial\phi/\partial x_2 \equiv u_{20}$, representing the near field of a turbulent flow occupying part or all of the half-space $x_2 < 0$. The motion is presumed incompressible so that the potential satisfies Laplace's equation. He does not treat the problem of determining u_{20} for a given turbulent flow: this has been studied approximately by Ffowcs Williams (1960), who indicates that the contribution from the turbulence/mean shear interaction greatly exceeds the direct contribution from the u_2-component within the turbulence, a result in conformity with the calculations of Lilley (1963) and others on the very similar problem of the pressure fluctuations on a solid surface adjacent to a turbulent flow. Phillips shows that the velocity potential satisfying Laplace's equation with the boundary condition $u_{20} = \cos(k_1x_1 + k_3x_3)$ is

$$\phi = -k^{-1}\exp(-kx_2)\cos(k_1x_1 + k_3x_3),$$

where $k^2 = k_1^2 + k_3^2$, and the general solution for the velocity potential in the half-space $x_2 > 0$ is

$$\phi = -\int dA(\mathbf{k})\, k^{-1} \exp(-kx_2) \exp(i[k_1 x_1 + k_3 x_3]),$$

where

$$u_{20} = \int dA(\mathbf{k}) \exp(i[k_1 x_1 + k_3 x_3])$$

and $dA(\mathbf{k})$ is a random function which can be thought of as a Fourier amplitude. (Here we use the usual notation in which x_2 is the direction approximately normal to the boundary of the turbulent flow and x_1 is the direction of mean motion, instead of Phillips's notation, in which x_1 is the direction normal to the boundary: conformity seems to be preferable to symmetry.) From this solution Phillips derives several expressions for the intensity spectra, microscales and so on in the irrotational region. Some of these will be quoted below, but the one most easily checked experimentally is that $\overline{u^2}$ should vary as x_2^{-4} for x_2 large compared with the wavelengths carrying most of the turbulent energy. It is assumed in the solution that the 'upwash' distribution u_{20} is equivalent to an array of *dipoles*, that is, that the source strength, or average value of u_{20} over the plane $x_2 = 0$, is zero at any instant. Liepmann (1962) has pointed out that a random 'whipping' of the shear layer as a whole would contribute a source term and invalidate the solution, but no such effect is apparent in the present results for a boundary layer or the results of Bradbury (1963) for a free jet in a moving stream. In Phillips's original paper, measurements by Townsend in a wake are reproduced, and a region where $\overline{u_1^2}$ varies as x_2^{-4} is identified. However, this region is in fact in the intermittent part of the flow and, whereas the contribution of the rotational fluctuations to $\overline{u_1^2}$ may have been fairly small, the above-mentioned condition for large x_2 was probably not satisfied. Liepmann (1962) remarks that the agreement with theory may have been largely coincidental, and the possibility of 'whipping' of the wake cannot be eliminated. While there is no reason whatsoever to doubt the accuracy of Phillips's theory it is useful to have numerical values for some of the constants and to establish regions of validity for the approximations in the theory. The several *ad hoc* investigations of the near field of circular jets, undertaken because of the practical interest in the effect of gas turbine exhausts on nearby parts of an aircraft structure, are not very helpful because the flow differs so greatly from the homogeneous plane flow treated by Phillips. Stewart (1956) indicated a formal solution for the *self-preserving* circular jet or axisymmetric mixing layer, but it involved associated Legendre functions of unknown properties and limited utility which he did not study further.

The present work was stimulated by an excellent confirmation of the x_2^{-4} law obtained by Bradbury (1963, 1965) in the highly advantageous experimental situation of a high-speed jet in a slow-moving stream: the irrotational fluctuations exceeded the free-stream turbulence of the wind tunnel for a considerable distance outside the flow, whereas Townsend's original measurements near a wake were hampered by the disappearance of the irrotational fluctuations into the background turbulence, about 0·09 % of the free-stream velocity. While the plane jet in a moving stream is not of much practical interest, the boundary layer is, and so some measurements have been made in the NPL 59 in. × 9 in. boundary-

layer tunnel (Bradshaw & Hellens 1964), which has a u_1-component turbulence level of about 0·04 % in the free stream. In order to ensure that the irrotational fluctuations due to the *roof* boundary layer did not influence the results, the measurements were made 4 ft. from the leading edge, where the boundary layer was only about 0·8 in. thick compared with the 9 in. height of the working section, at a Reynolds number $U_1 x/\nu$ of about 3×10^6 and in zero pressure gradient. Some further measurements have been made, at the same station and about the same

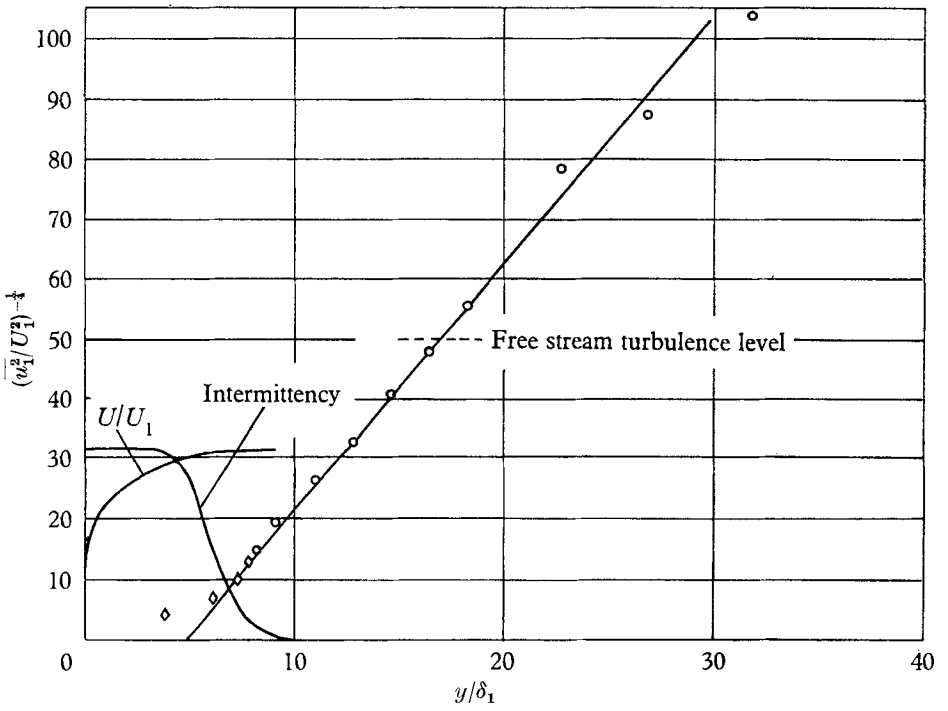

FIGURE 1. Longitudinal-component intensity near constant-pressure boundary layer. ○, Present experiment $U_1\delta_1/\nu = 7200$; ◇, Klebanoff $U_1\delta_1/\nu = 11{,}500$.

value of $U_1 x/\nu$, in a strongly retarded equilibrium boundary layer with $U_1 \propto x^{-0.255}$ (Bradshaw 1965). The transformer-coupled constant-current hot-wire apparatus (Ferriss 1963) was used and the noise level of the electronics was always negligible except for pick-up at the mains frequency, 50 c/s.

Dumas (1964) has published some measurements of the irrotational fluctuations near a boundary layer in zero pressure gradient which extend the results reported by Favre, Gaviglio & Dumas (1957) and are in good agreement with the present work.

2. The u_1-component intensity and the x_2^{-4} law

The u_1-component intensity measurements in zero pressure gradient (figure 1) fall close to the line $\overline{u_1^2}/U_1^2 = 0{\cdot}0034(y/\delta_1 - 4{\cdot}8)^{-4}$ for large values of y. It should be noted that the last three points were obtained as small differences between the total mean-square intensity and the value in the centre of the tunnel, so that the

proximity of these points to the line is largely a matter of luck. The measurements at small x_2 join up well with the results of Klebanoff (1955). The intensity measurements in the boundary layer with $U_1 \propto x^{-0.255}$ are shown in figure 2: the

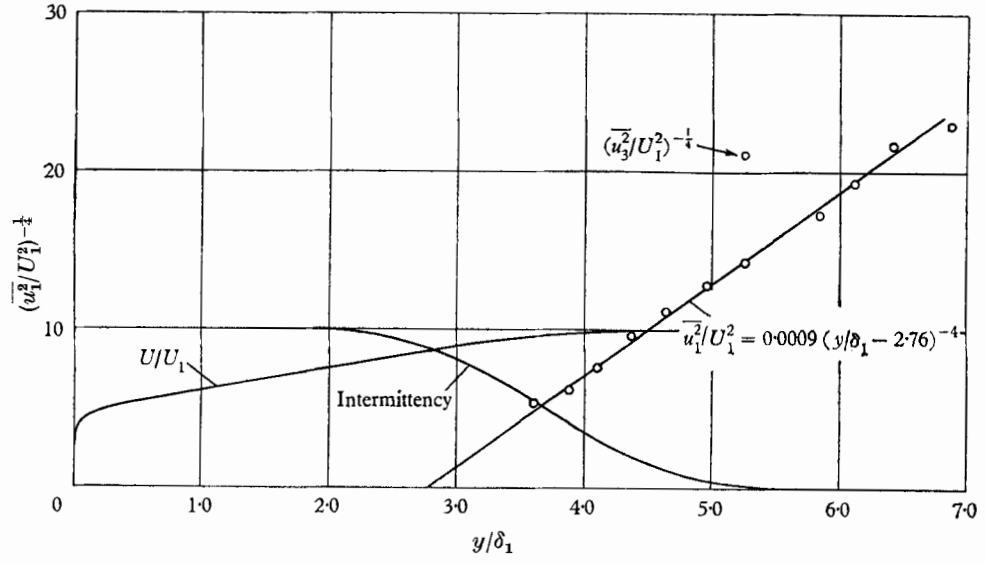

(*a*)

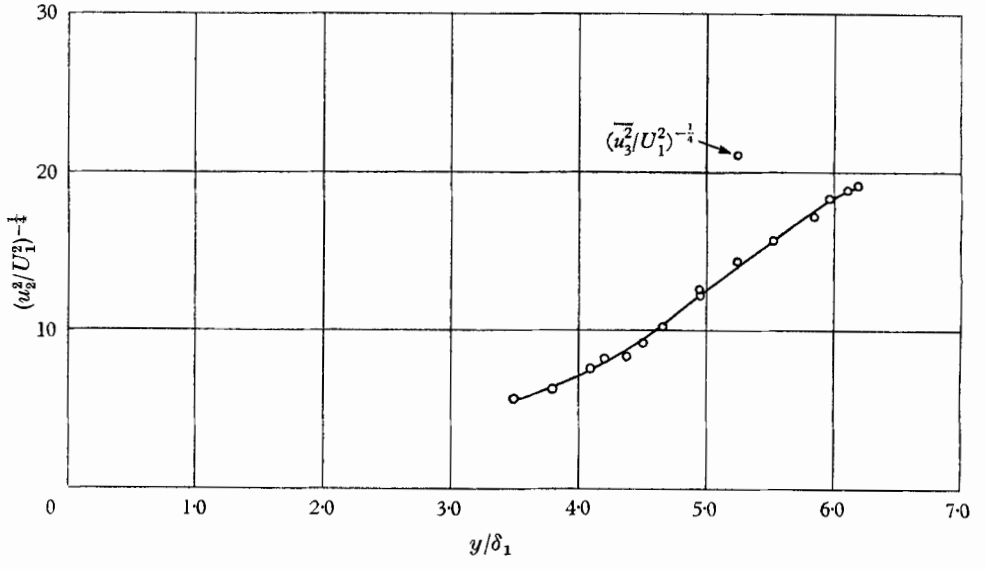

(*b*)

FIGURE 2 (*a*) Longitudinal-component intensity near boundary layer with $U_1 \propto x^{-0.255}$. (*b*) Normal-component intensity near boundary layer with $U_1 \propto x^{-0.255}$.

u_2 measurements and the single u_3 point have been corrected by subtracting a spurious signal due to eddy shedding from the prongs of the hot wire probe. The measurements become unreliable near the centre line of the tunnel because of the irrotational field of the roof boundary layer, and a rather conjectural 'free

stream' level has been subtracted from each component. Therefore the results are not as reliable a verification of the x_2^{-4} law as the measurements in zero pressure gradient, but the equations of the best straight line through the u_1 measurements is shown in figure 2(*a*). The intercept on the y-axis has no physical significance: in particular, it cannot strictly be identified with the region of the layer that contributes most to the irrotational field, although in both boundary layers it is, plausibly, at about 0·8 of the distance from the surface at which the intermittency is 0·5 (the average position of the turbulence front). This is because the x_2^{-4} law becomes valid only at distances from the plane $x_2 = 0$ which are large compared with the wavelengths of the energy-containing motion in the plane $x_2 = 0$, so that the intercept is ill-defined and subject to a most-probable error of the order of the aforementioned wavelengths. Moreover, *any* plane can be chosen as $x_2 = 0$ for the purpose of the theory and at a sufficient distance from such a plane the intensity will vary as x_2^{-4}, so that $x_2 = 0$ is again shown to be essentially ill-defined.

Measurements of the u_2- and u_3-components have not been made in the present tests in zero pressure gradient, because the mean-square intensities of these components in the free stream of the wind tunnel are about six times the intensity of the u_1-component in the free stream, so that the irrotational fluctuations would be difficult to discern above the background level, quite apart from the usual difficulties with eddy shedding from the probe. Phillips's theory gives the relation $\overline{u_2^2} = \overline{u_1^2} + \overline{u_3^2}$, and Grant's (1958) correlation measurements show that the u_2-component correlations in the outer part of the turbulent flow are roughly equal for r_1 and for r_3 separations, so that to a first approximation the irrotational field is axisymmetric about the x_2-axis and the field is thus completely described by the u_1-component. (Here 'axisymmetric' means only 'invariant to rotation about the axis' and does *not* include invariance with respect to reflections in the x_1x_3 plane as Batchelor's (1956) definition does. Also, in this paper 'two-dimensional' refers to (k_1, k_3) spectra in the sense that 'one-dimensional' refers to k_1 spectra: it does not mean 'independent of x_3'.)

Measurements of u_2-component correlations have not been made within the retarded boundary layer, but it is immediately clear that $\overline{u_1^2} \neq \overline{u_3^2}$ in the irrotational field so that the latter is far from axisymmetric in this case. The reasons for this will be discussed below, but they do not reflect upon the deduction from Grant's measurements that the irrotational field of the boundary layer in zero pressure gradient is roughly axisymmetric, and it is probable that this deduction is valid for boundary layers in moderate pressure gradients also. Since the assumption of axisymmetry enables us to derive a surprisingly large amount of information from a small quantity of experimental data, we proceed to discuss this special case of Phillips's theory.

3. Wave-number and frequency spectra in an axisymmetric field: one-dimensional and two-dimensional spectra

Phillips's analysis is formulated in terms of the two-dimensional wave-number spectrum of the normal-component fluctuations, $\Phi_{22}(k_1, k_3)$. In the most general case, this can be obtained experimentally only as the two-dimensional Fourier

transform of the correlation $R_{22}(r_1, 0, r_3)$ for all r_1, r_3. If the irrotational field is axisymmetric, R_{22} and Φ_{22} are functions only of the magnitude, and not of the direction, of the separation and wave-number vectors respectively, and can be written $R_{22}(r)$ and $\Phi_{22}(k)$ where $r = \sqrt{(r_1^2+r_3^2)}$ and $k = \sqrt{(k_1^2+k_3^2)}$. Thus the field is completely determined by, for instance, a measurement of $R_{22}(r_1, 0, 0)$. If the irrotational field obeys Taylor's hypothesis and is convected past the measurement point as a rigid pattern, then $R(r_1, 0, 0) = R(U_c\tau)$ where the convection velocity U_c is implied to be independent of wave-number but need not be the same as the fluid velocity, and the one-dimensional wave-number spectrum

$$\phi(k_1) \equiv \int_{-\infty}^{\infty} \Phi(k) dk_3$$

can be obtained as the frequency spectrum $\phi(\omega/U_c)$, which is much easier to measure than a spatial correlation, particularly in the low-intensity irrotational field. The assumption of axisymmetry in zero pressure gradient has been discussed above: the assumption of the truth of Taylor's hypothesis is at least as justified for the irrotational field as for the turbulent flow itself, and the inaccuracy of both assumptions is likely to be much less than the inaccuracy of the $R(r_1, 0, r_3)$ measurements required to justify them. Correlations with $(r_1, 0, 0)$ separation would be extremely difficult to make because of the effect of the wake of one hot wire probe on the other.

The following discussion is based on measurements of the frequency spectrum $\phi(\omega/U_c)$, which is assumed to be equal to the one-dimensional wave-number spectrum $\phi(k_1)$. The value of U_c can actually be deduced from the frequency spectrum measurements and some of the results of Phillips's theory.

4. The convection velocity and the pressure fluctuations

In the appendix it is deduced from Phillips's theory that the leading terms of the normal-component spectrum in the plane $x_2 = 0$ can be written $\theta_2 k^2$ where θ_2 is a constant given directly by the behaviour of the longitudinal-component spectrum $\phi_{11}(k_1)$ at small k_1 if the convection velocity U_c is known, since

$$\phi_{11}(k_1) \sim \theta_2 k_1^2/x_2 \sim \theta_2 \omega^2/x_2 U_c^2.$$

Thus it is necessary, and not merely desirable, to know the convection velocity. It can in fact be deduced from the behaviour of $\phi_{11}(\omega/U_c)$ at large ω by finding the best fit to the exponential cut-off. A suitable graphical method is to plot

$$x_2 \partial \log \phi_{11}/\partial x_2,$$

(theoretically equal to $-\frac{1}{2} - 2\omega x_2/U_c$: see appendix, (13*a*) and (15*a*)) against x_2 and fit the best straight line to the points: at first sight this might appear to involve giving a physical significance to the plane $x_2 = 0$, but in fact the approximations involved in the analytical form imply that it is valid only for large x_2, like the x_2^{-4} law for the intensity, and therefore does not depend critically on the origin of x_2. The determination of convection velocity from single-point measurements is not possible for general turbulent flows: in the particular case of the irrotational field we are in effect assuming that the conditions at $x_2 = 0$ are

known so that measurements of $\phi(\omega)$ at different x_2 amount to a degenerate filtered space correlation, which resolves the paradox.

The pressure-fluctuation spectrum in the irrotational field, which it is interesting to compare with the spectrum at the wall, is obtained from the unsteady form of Bernoulli's equation,

$$\overline{p}+p+\tfrac{1}{2}\rho|u|^2=\rho(\partial\phi/\partial t)$$

(or from Euler's equation using the conditions of irrotationality $\partial u_i/\partial x_j=\partial u_j/\partial x_i$), making the assumption that a unique convection velocity exists so that

$$\partial/\partial t=-U_c(\partial/\partial x),$$

where U_c is not necessarily equal to U_1. We find

$$-p/\rho=(U_1-U_c)\,u_1+\tfrac{1}{2}(u_1^2+u_2^2+u_3^2)$$

on discarding the mean part $\overline{p}+\frac{1}{2}\rho U_1^2$. Physically this equation, which is of course valid even if the irrotational field is not axisymmetric, means that the pressure fluctuation is partly the result of dynamic-pressure fluctuations directly due to the irrotational velocity fluctuations, and partly the result of flow at speed U_1 over an equivalent 'wavy wall' moving at the convection velocity U_c. (The 'wavy wall' is the displacement surface, which is not in general the same as the laminar–turbulent interface although both are convected at approximately the speed of the large eddies.) Even if the convection velocity is as high as $0{\cdot}95\,U_1$—and both the experimental results presented below and the wall-pressure measurements of other workers suggest that it is probably less—the wavy-wall term greatly exceeds the quadratic term since $(\overline{u_1^2})^{\frac{1}{2}}/U_1<0{\cdot}002$ in the irrotational region (actually the quadratic term is likely to be of the same order as the error incurred by assuming $\partial/\partial t=-U_c\partial/\partial x$, and we have already ignored this error). Thus the two-dimensional pressure-fluctuation spectrum is nearly the same shape as the u_1-component spectrum. (For another discussion of the wavy-wall concept see Liepmann (1954): unfortunately Liepmann's analytical results are based on the assumption $\theta(k)=$ constant, which does not satisfy the continuity condition.)

It follows from 15(*b*) and the above relation between velocity and pressure fluctuations that the spectrum of the pressure fluctuations outside the boundary layer should tend to zero as ω^2 for small ω: strictly the spectral density at zero frequency takes a non-zero value because the contribution of the quadratic terms behaves approximately as a convolution integral which is bound to be finite at zero frequency, but we have shown that the quadratic contribution is very small. Since it is difficult to imagine circumstances in which the low wave-number contributions to the pressure fluctuation could differ markedly in character between the irrotational field and the wall—even at the peak of the spectra shown in figure 3 the wavelength is about four times the distance from the measurement point to the wall—it follows that the wall-pressure spectrum should also have a region of ω^2 dependence, possibly with a noticeable contribution very near $\omega=0$ from the quadratic terms. This is of course the conclusion reached by Lilley (1963) and others, by arguments concerning the relative importance of the 'turbulence/mean shear' and 'turbulence/turbulence' (quadratic) terms in the

Poisson equation for the pressure. We have carefully refrained from invoking these arguments directly although they are closely related to the considerations above. Corcos (1964), using the pressure–velocity correlation data of Wooldridge

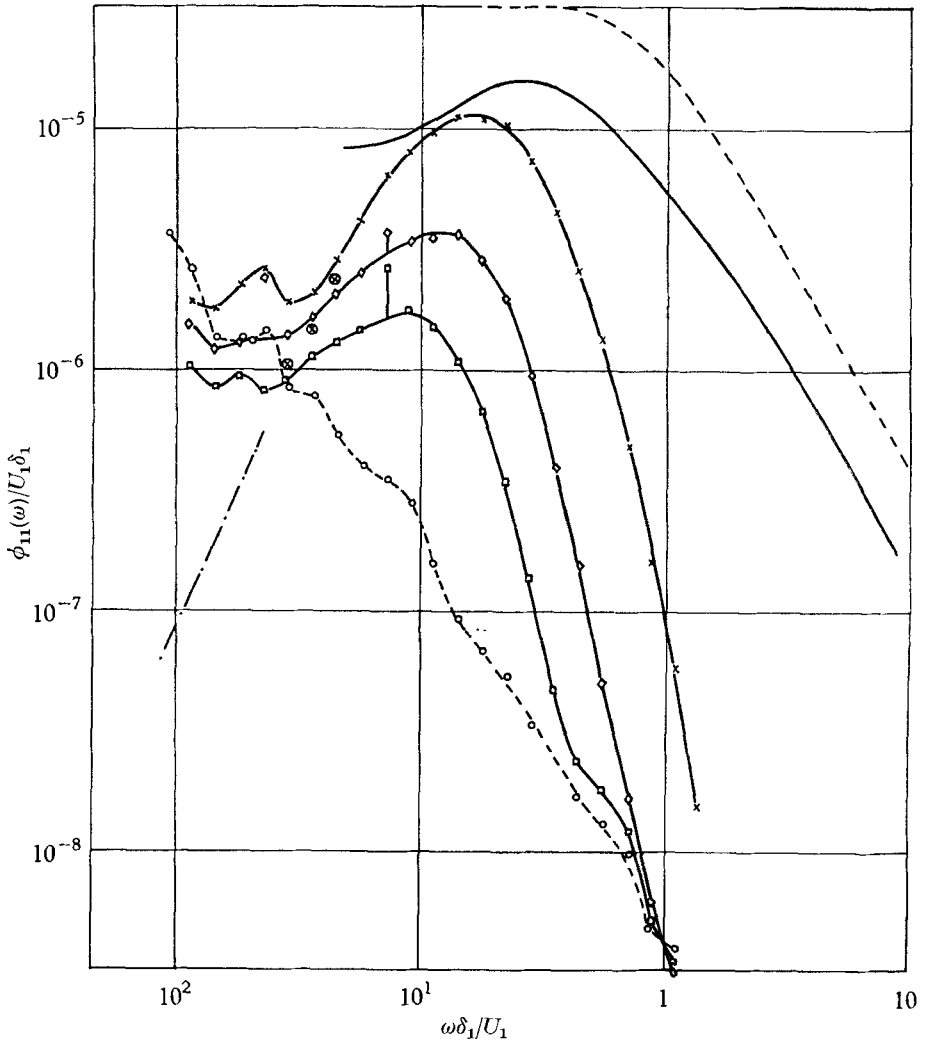

FIGURE 3. Frequency spectrum of longitudinal component near constant-pressure boundary layer. ×, $y/\delta_1 = 10{\cdot}3$; ⊗, $y/\delta_1 = 10{\cdot}3$ tunnel turbulence subtracted; ◇, $y/\delta_1 = 13{\cdot}3$; □, $y/\delta_1 = 16{\cdot}4$; ---○---, tunnel turbulence. ——, wall-pressure spectrum (Serafini), and -----, ϕ_{22} at $y/\delta_1 = 4$ (Klebanoff) (arbitrary vertical positions); ·—·—·, asymptotic ω^2 dependence at $y/\delta_1 = 10{\cdot}3$.

& Willmarth (1962), has derived a value for the 'turbulence/mean shear' contribution to the wall-pressure intensity which is much less than the measured intensity, and concludes that the turbulence/turbulence terms are not small, so that the matter cannot be regarded as settled. As is well known, experiments on wind-tunnel boundary layers totally fail to verify the existence of an ω^2 region in the spectrum of the wall-pressure fluctuations, measurements in the NPL

boundary-layer tunnel (Wills 1964) being no exception: the scatter between the results of different workers for the low-frequency end of the spectrum is enormous, indicating that extraneous influences are at least partly responsible. Certainly the tunnel turbulence is high enough to contribute noticeably to the near-field velocity fluctuations, particularly at low frequency, but it is *not* large enough to explain the apparent discrepancy between the low-frequency behaviour of the near-field pressure spectrum calculated from (15) and the behaviour of the measured wall-pressure spectra. If, however, part of the tunnel 'turbulence' consisted of sound waves, then a velocity fluctuation intensity u_1^2 would correspond to a pressure fluctuation intensity $\rho^2 a_0^2 u_1^2$ which is several orders of magnitude greater than $\rho^2(U_1 - U_c)^2 u_1^2$ at the speeds of the present experiment. In fact, the observed low-frequency behaviour of the pressure-fluctuation spectra in the boundary-layer tunnel could be roughly accounted for if only about one-tenth of the low-frequency tunnel 'turbulence' consisted of noise and Wills (1965) has recently measured spatial correlations in narrow frequency bands which confirm that a large part of the low-frequency pressure fluctuation consists of sound waves travelling *upstream*, presumably from the diffuser of the wind tunnel. The only wall-pressure spectra which have a detectable ω^2 region are the wall-jet measurements of Lilley & Hodgson (1960) (confirmed by measurements at NPL) and measurements on a glider wing, also by Hodgson (1962): in both these environments the external noise level was probably low compared with the pressure fluctuations.

It is worth remarking explicitly that the two-dimensional u_1-component spectrum is not axisymmetric, so that an axisymmetric irrotational field does *not* imply an axisymmetric pressure-fluctuation field: it is quite compatible with actual measurements of pressure-fluctuation correlations with separation in the r_3 direction.

5. Frequency spectra: experimental results

(i) *Zero pressure gradient*

The behaviour of the experimental $\phi_{11}(\omega)$ spectra near zero frequency is obscured by the free-stream turbulence (figure 3) and it is clear that subtracting the free-stream spectral density from the measured spectral density is rather inaccurate: it is noticeable that the roughly constant value to which the measured spectra tend at low frequency *decreases* by a factor of about 2 as y/δ_1 increases from 10·3 to 16·4 (x_2/δ_1 increasing from about 5·5 to 11·6, again about a factor of 2), but since the spectral density of the free-stream turbulence, measured on the centre line of the tunnel, lies midway between the two extremes it is not possible to say whether this represents any significant trend. The line shown as the asymptotic variation at $y/\delta_1 = 10{\cdot}3$ implies $\theta_2/(U_1^2\delta_1^4) = 2{\cdot}1 \times 10^{-3}$ from equation (15*b*) (taking $U_c = 0{\cdot}9U_1$ and noting that $\phi(\omega) = \phi(k_1/U_c) + \phi(-k_1/U_c)$).

The behaviour of the spectra at the highest frequencies is again influenced by the tunnel turbulence but it is seen that the cut-off is much more rapid than the cut-off of Klebanoff's ϕ_{22} spectrum at $y/\delta_1 = 4$, or the wall-pressure spectrum, which are also shown in figure 3 at *arbitrary* vertical positions on the graph.

The microscales were calculated from the second moments of the frequency spectra. At $y/\delta_1 = 10{\cdot}3$ and $13{\cdot}3$ the microscales are $2{\cdot}72\delta_1$ and $4{\cdot}8\delta_1$ respectively, assuming $x_2 = 0$ at $y/\delta_1 = 4{\cdot}8$ and $U_c/U_1 = 0{\cdot}9$. The theoretical values for the

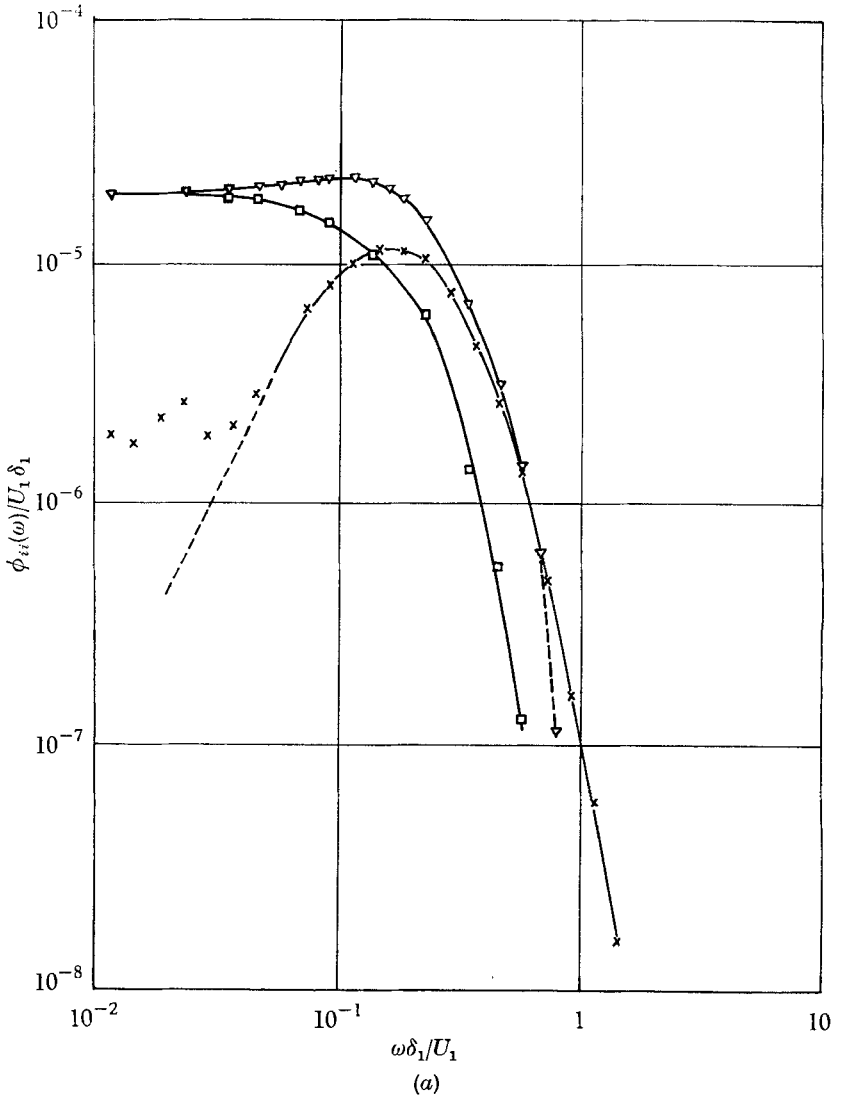

FIGURE 4. For legend see p. 220.

axisymmetric case, $\lambda = 2(15)^{-\frac{1}{2}}x_2$, are $2{\cdot}85\delta_1$ and $4{\cdot}4\delta_1$ respectively. The agreement is reasonable, and provides further evidence in favour of the assumption of axisymmetry although the test is not a severe one.

The u_2 and u_3 spectra calculated from the u_1 spectrum on the assumption of axisymmetry are shown in figures 4(*a*)–4(*c*), and the $\Phi_{22}(k)$ spectra are shown in figure 5. The difference between the three $\Phi_{22}(k)$ spectra at low wave-number is greater than the expected factor $\exp(-2kx_2)$, and must be attributed to experimental errors at low frequencies. Using the results at $y/\delta_1 = 10{\cdot}3$, the three

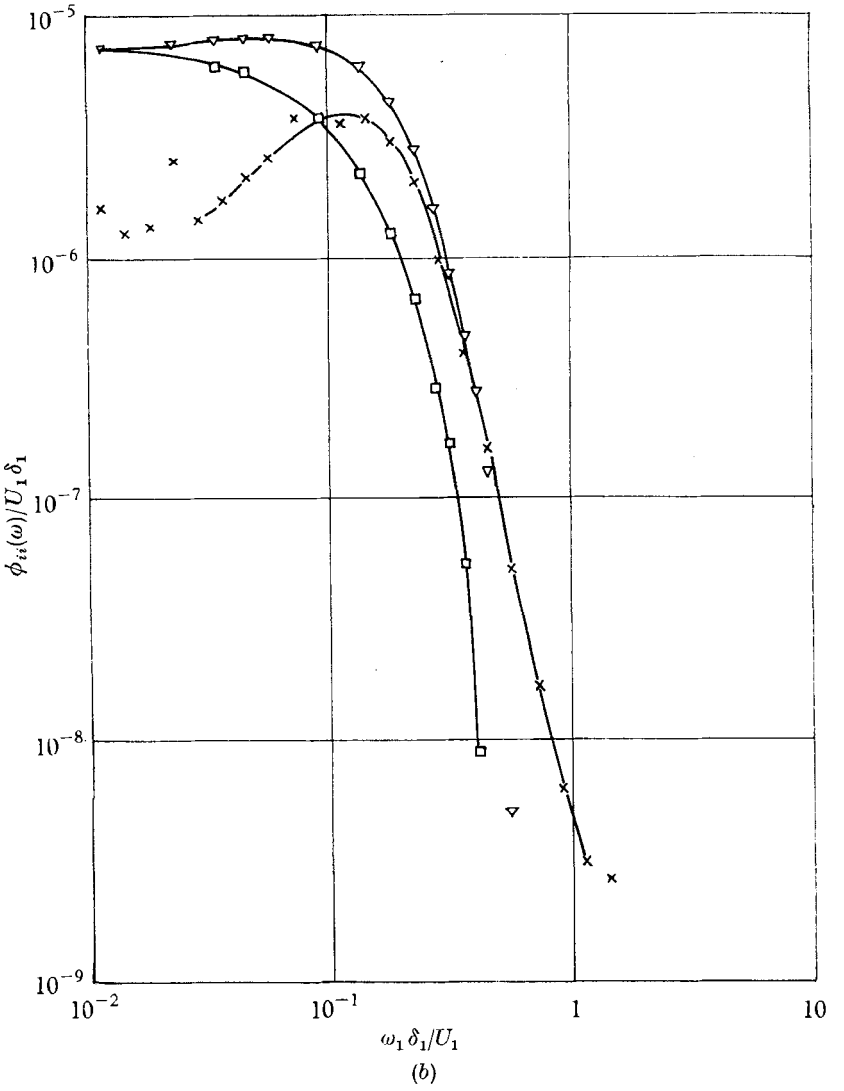

FIGURE 4 (*cont.*). For legend see p. 220.

methods of obtaining θ_2, the constant in the expression $\theta(k) \sim \theta_2 k^2$ for the low wave-number behaviour of the u_2 spectrum in the plane $x_2 = 0$, give

$$\operatorname*{Lt}_{k\to 0}\left\{\frac{1}{k^2}\Phi_{22}(k)\right\} = 8{\cdot}75\times 10^{-4}U_1^2\delta_1^4,$$

$$\operatorname*{Lt}_{k_1\to 0}\left\{\frac{x_2}{k_1^2}\phi_{11}(k_1)\right\} = 2{\cdot}13\times 10^{-3}U_1^2\delta_1^4,$$

$$\operatorname*{Lt}_{k_1\to 0}\{2x_2^3\phi_{22}(k_1)\} = 3{\cdot}4\times 10^{-3}U_1^2\delta_1^4.$$

All three figures are affected by the difficulty of allowing for the effect of tunnel turbulence on $\phi_{11}(k_1)$ at small k_1: the first figure is the most reliable and the others strongly suggest that the best choice for the notional 'plane of origin' of the

irrotational field, $x_2 = 0$, is further from the surface than the distance $4{\cdot}8\delta_1$, deduced from the intensity measurements of figure 1, which was used in the calculations. Probably the slope of the straight line in figure 1 is affected by the increasing validity of the condition for the existence of an x_2^{-4} law, $x_2/\delta_1 \gg 1$. The function $\theta(k) \equiv \Phi_{22}(k) \exp 2kx_2$ varies as k^2 up to a wave-number $k\delta_1$ of

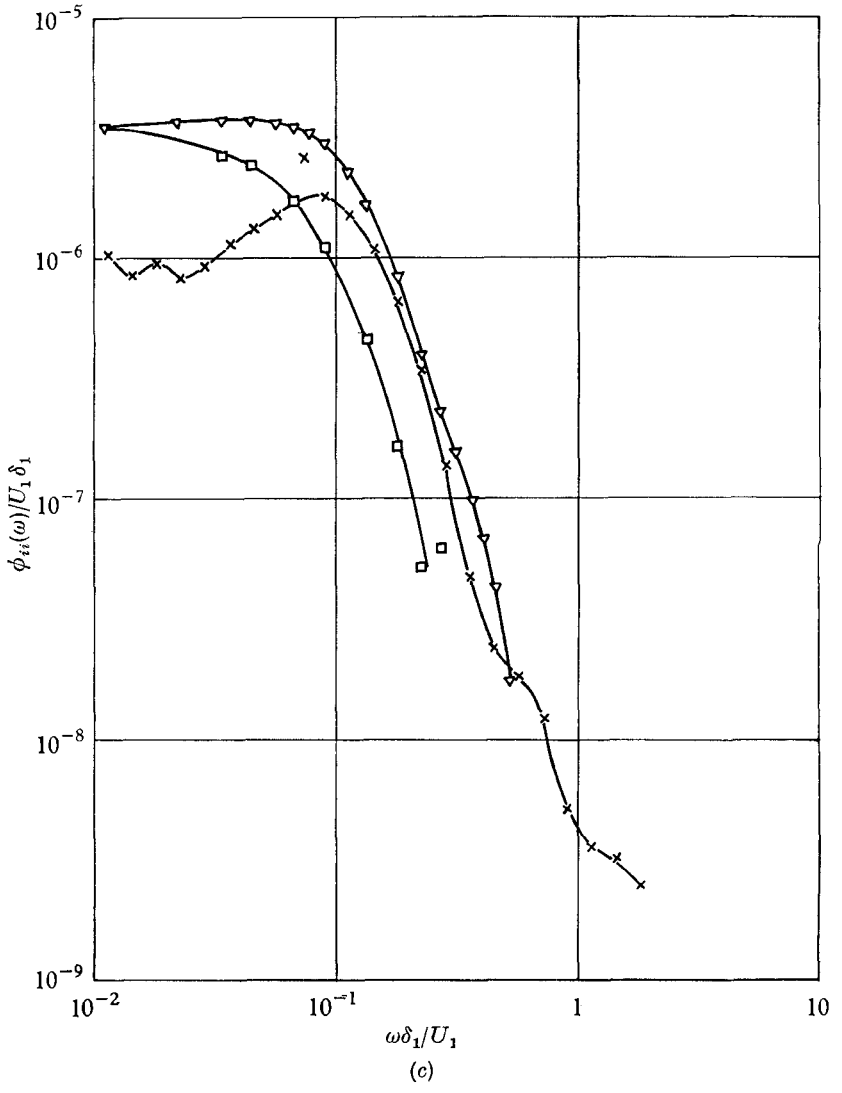

FIGURE 4. Frequency spectra near constant-pressure boundary layer ×, ϕ_{11} (measured); ▽, ϕ_{22} and, □, ϕ_{33} calculated from ϕ_{11} spectrum. (*a*) $y/\delta_1 = 10{\cdot}3$; (*b*) $y/\delta_1 = 13{\cdot}3$; (*c*) $y/\delta_1 = 16{\cdot}4$.

slightly more than 0·1 and then begins to flatten out, but increases sharply for $k\delta_1 > 0{\cdot}5$ (well past the peak of the $\Phi_{22}(k)$ spectrum): this improbable behaviour may be partly due to numerical integration errors in the computer program, but it is more likely to be caused by inaccuracy of measurement of $\phi_{11}(\omega)$ at high frequencies. The $\phi_{11}(k_3)$ spectrum, which is identical with the $\phi_{33}(k_1)$ spectrum, is

qualitatively like the k_3 surface pressure fluctuation spectra measured by Wills (1965).

The convection velocity could in principle be found from a comparison of the actual u_1-component spectrum cut-off at high ω with the asymptotic result $\phi_{11} \propto k_1^{\frac{5}{2}} x^{-\frac{1}{2}} \exp(-2k_1 x_2)$, but it is more satisfactory to use graphs of ϕ_{11} against

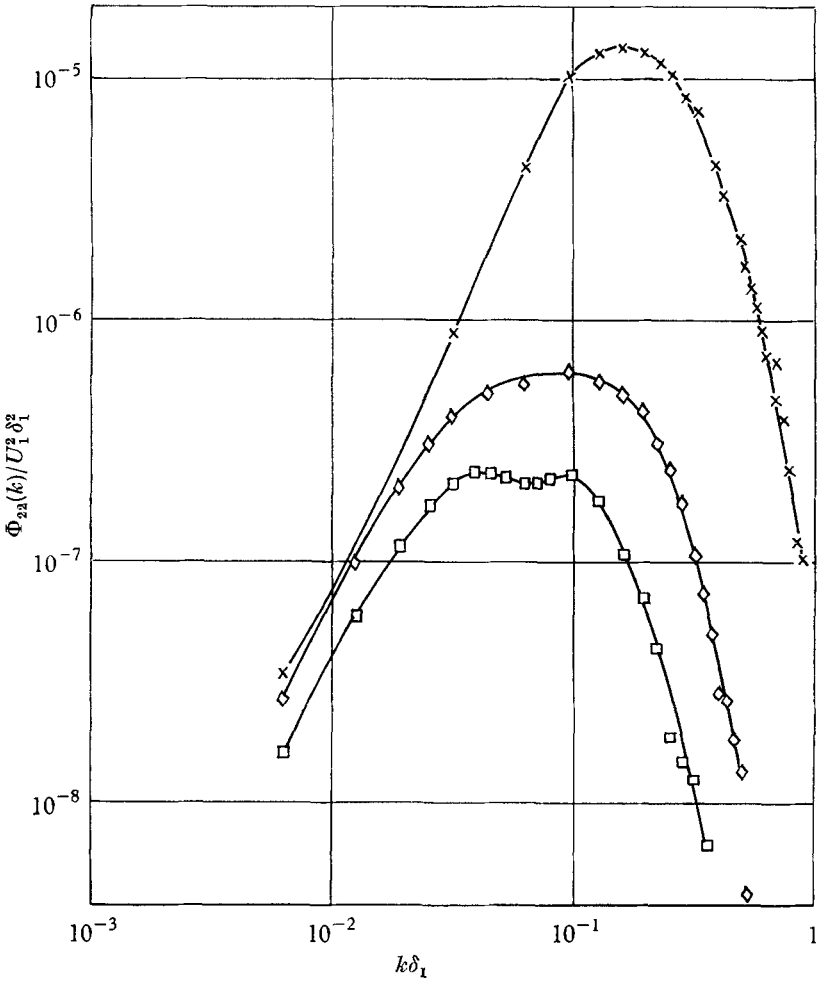

FIGURE 5. Wave-number-magnitude spectra near constant-pressure boundary layer. ×, $y/\delta_1 = 10{\cdot}3$; ◇, $y/\delta_1 = 13{\cdot}3$; □, $y/\delta_1 = 16{\cdot}4$.

x_2 for different medium frequencies where $\theta(k) \sim k^2$, and to compare them with the same asymptotic result. Separate measurements of the spectral density were made in the form of traverses in the y-direction at several fixed frequencies, and the free-stream spectral density (taken as that at the largest value of y, about 3 in. or $30\delta_1$) was subtracted from the results. Then for each ω, $x_2(\partial \log \phi/\partial x_2)$ was plotted against x_2 taking $x_2 = 0$ at $y/\delta_1 = 4{\cdot}8$, and the best straight line with an intercept of $-\frac{1}{2}$ on the vertical axis was fitted to the result. In most cases the plotted slopes were extremely scattered, especially at the larger values of y and

the extreme values of frequency where the free-stream spectral density overwhelmed the readings. The results for U_c are shown in figure 6: in all cases except that at the lowest frequency, the best straight line was chosen irrespective of the plausibility of the resulting value for U_c so that the consistency of the results is

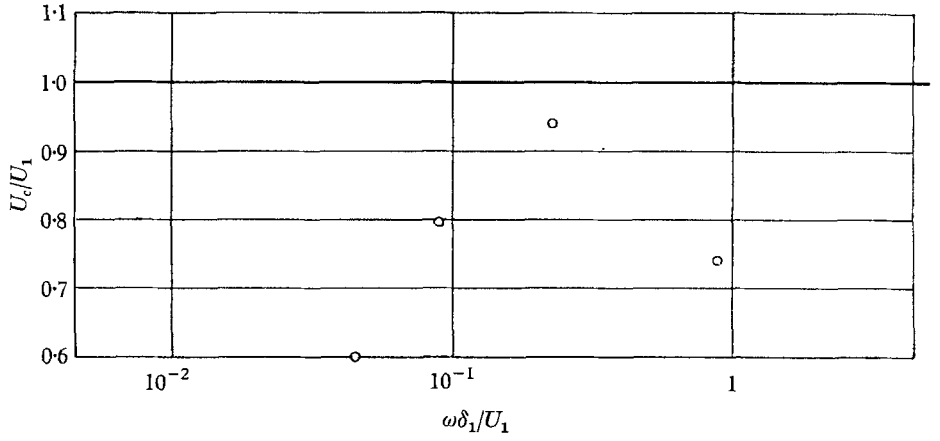

FIGURE 6. Convection velocity, obtained from $\phi_{11}(\omega, x_2)$ at constant ω, near constant-pressure boundary layer.

surprisingly good. The apparent increase of convection velocity with frequency is unlikely to be significant, although it is perfectly plausible when one realizes that the high-frequency contributions to the irrotational field probably come from the turbulence in the 'bulges' in the intermittent region of the flow rather than the more intense, but more distant, turbulence near the wall. The accuracy of the measurements is likely to be best within the range $0{\cdot}1 < \omega\delta_1/U_1 < 0{\cdot}3$, where the spectral density is greatest, and we conclude that the convection velocity of the near-field irrotational fluctuations may be as high as $0{\cdot}9U_1$ compared with the value of $0{\cdot}8U_1$ usually quoted for the wall-pressure fluctuations. The root-mean-square pressure fluctuation at $y/\delta_1 = 10{\cdot}3$, just outside the outermost boundary of the turbulent flow, can then be calculated from (15) as about $4 \times 10^{-4} . \frac{1}{2}\rho U_1^2$ or $0{\cdot}15\tau_w$ compared with about $2{\cdot}6\tau_w$ on the surface. If the spectra of figure 3 are now regarded as pressure-fluctuation spectra, the 'arbitrary' position of Serafini's spectrum is approximately a factor 100 lower than the correct position: the actual factor is proportional to $(U_1 - U_c)^2$ and therefore highly uncertain.

(ii) *Adverse pressure gradient*, $U_1 \propto x^{-0{\cdot}255}$

In the retarded equilibrium boundary layer with $U_1 \propto x^{-0{\cdot}255}$, the turbulent intensity, and more particularly the spectral density at low frequencies, is high enough for direct measurements of the u_2- and u_3-components of the irrotational fluctuations to be made, and the spectra of all three components at $y/\delta_1 = 5{\cdot}25$ (approximately the outer edge of the intermittently turbulent region) are shown in figure 7. It is clear that the u_2 spectrum is not axisymmetrically related to the u_1 spectrum, nor is the u_3-component intensity equal to the u_1-component intensity (in fact it is very much smaller). This appears to cast doubt on the

assumption of axisymmetry as a first approximation in the boundary layer in *zero* pressure gradient. However, there is indirect evidence that the $R_{22}(r, 0, 0)$ and $R_{22}(0, 0, r)$ correlations within the retarded boundary layer may be very different from Grant's measurements in a jet mixing layer reported by Bradshaw, Ferriss & Johnson

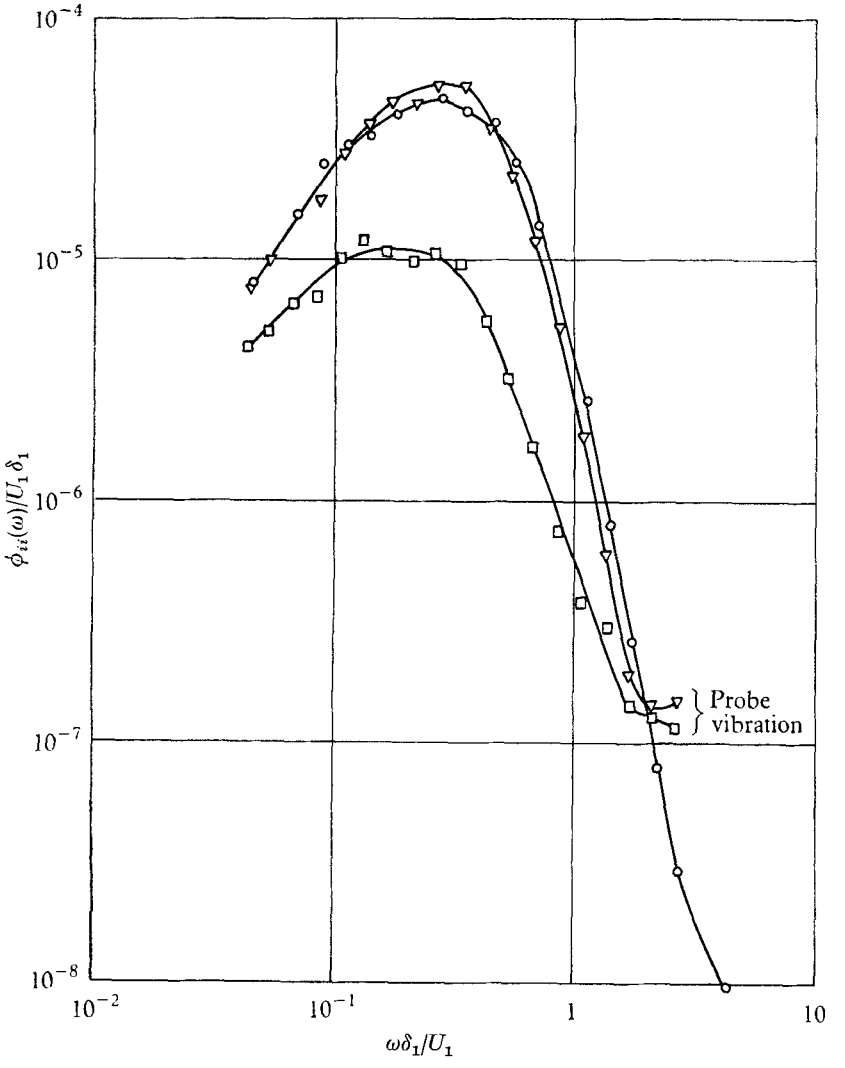

FIGURE 7. Frequency spectra near boundary layer with $U_1 \propto x^{-0.255}$. $y/\delta_1 = 5{\cdot}25$. ○, ϕ_{11}; ▽, ϕ_{22}; □, ϕ_{33}.

(1964), which showed that the $R_{22}(r, 0, 0)$ correlation had a pronounced oscillation which was absent from the $R_{22}(0, 0, r)$ correlation, the integral scales in the region of maximum turbulence intensity being respectively 0·015 and 0·038 times the distance from the point of origin of the mixing layer. General observations of the shear stress distribution and the intensity spectra within the retarded boundary layer suggest that its turbulence structure may be much closer to the

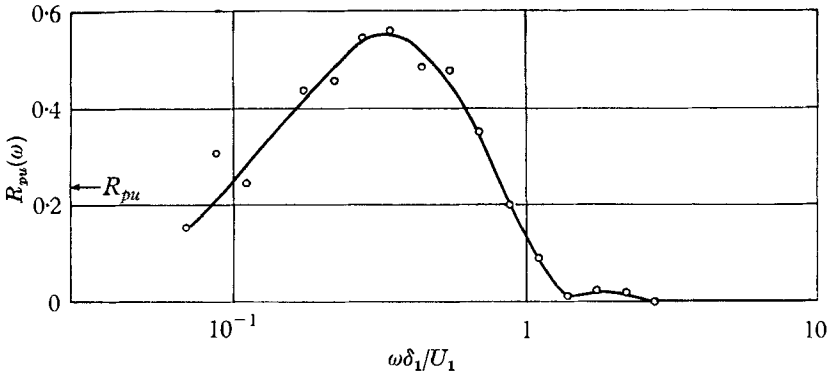

FIGURE 8. Surface-pressure/velocity correlation coefficient in narrow frequency bands: $U_1 \propto x^{-0\cdot255}$, $y/\delta_1 = 5\cdot25$.

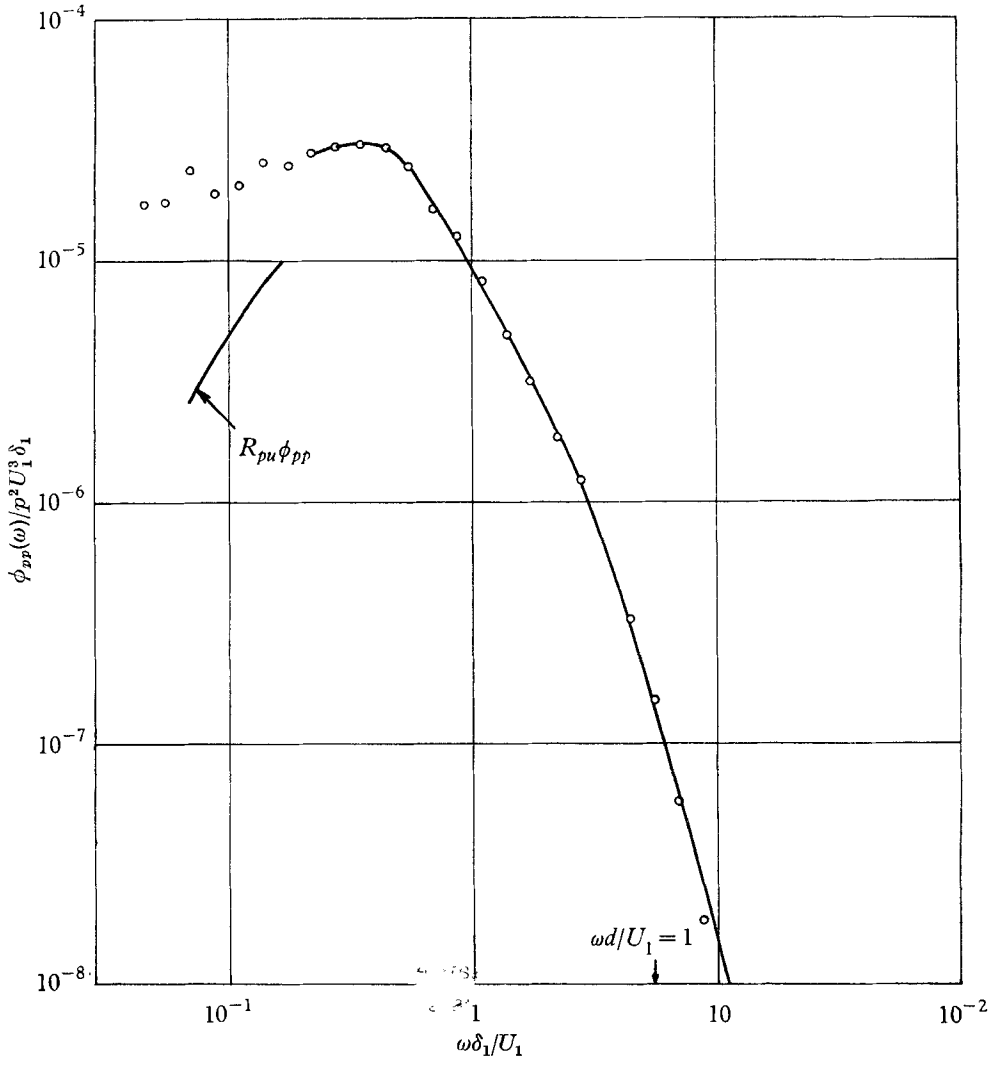

FIGURE 9. Surface-pressure fluctuation spectrum: $U_1 \propto x^{-0\cdot255}$.

jet mixing layer than to the boundary layer in zero (or moderately adverse) pressure gradient. In order to clear the matter up completely one would like to have measurements of the u_2- and u_3-component intensities in the irrotational field of the boundary layer in zero pressure gradient but, for reasons mentioned above, these would be very difficult to obtain.

The spectra in the retarded boundary layer are clearly approaching an ω^2 dependence at the lowest frequencies but unfortunately the lowest frequency of the spectrum analyser, 16 c/s, corresponds to $\omega\delta_1/U_1 = 0{\cdot}05$ compared with 0·01 in the boundary layer in zero pressure gradient. Another disadvantage of the greater thickness of the retarded boundary layer is that the shallow height of the tunnel prevented measurements of spectra being made over a sufficiently large range of y/δ to define the convection velocity. The wall-pressure convection velocity measurements by Bradshaw (1965) suggest that it would be significantly less than in zero pressure gradient, as do the measurements of a rather arbitrarily defined convection velocity within the turbulent fluid by Bradshaw (1966).

The most interesting feature of the measurements in the retarded layer is the very strong correlation between the surface pressure fluctuation and the u_1-component fluctuation in the irrotational field. The correlation coefficient in narrow frequency bands is plotted in figure 8: it does not rise to unity, even at the lowest frequencies, but it seems very likely that it would so do if the contribution of sound waves to the pressure fluctuation could be eliminated. The surface pressure fluctuation spectrum is shown in figure 9. It has a distinguishable peak: the spectral density at the lowest frequencies approaches nearly the same value as in the measurements of Wills (1964) made in zero pressure gradient in the same tunnel, an additional demonstration that the lowest-frequency fluctuations are peculiar to the tunnel and not the boundary layer. $R_{pu}\phi_{pp}$ simulates the true low-frequency spectrum.

6. Conclusions

(1) The mean square intensity of the longitudinal-component fluctuation in the irrotational region of a constant-pressure boundary layer is given by $\overline{u_1^2}/U_1^2 = 0{\cdot}0034(y/\delta_1 - 4{\cdot}8)^{-4}$ for $y/\delta_1 > 10$ at $U_1\delta_1/\nu = 7200$, corresponding to $\overline{u_1^2}/u_\tau^2 = 2{\cdot}6(y/\delta_1 - 4{\cdot}8)^{-4}$: and in a retarded equilibrium boundary layer with $U_1 \propto x^{-0{\cdot}255}$, by $\overline{u_1^2}/U_1^2 = 0{\cdot}0009(y/\delta_1 - 2{\cdot}76)^{-4}$.

(2) If the irrotational field is symmetrical about the x_2-axis, an assumption supported, for the case of the constant-pressure boundary layer, by correlation measurements within the turbulent flow, the longitudinal wave-number spectrum $\phi_{11}(k_1)$ of the longitudinal component fluctuation determines the wave-number-magnitude spectrum $\phi(k)$ of the normal-component fluctuation in the notional plane of origin of the irrotational field, either directly through an integral relation or indirectly through Fourier and Hankel transforms. Asymptotic relations for the one-dimensional spectra at large distances from the plane of origin can be derived from these relations or special cases of them, and the leading term in $\theta(k)$ can be deduced directly from the low wave-number behaviour of $\phi_{11}(k_1)$.

(3) If the existence of a unique convection velocity U_c, not necessarily equal

to the free-stream velocity U_1, is assumed, the frequency spectrum of the longitudinal component $\phi_{11}(\omega)$ determines the whole irrotational field, and the convection velocity can be deduced from this frequency spectrum and the above asymptotic relations. The experimental value is very roughly $0{\cdot}9U_1$ for the constant-pressure boundary layer.

(4) If $U_c \neq U_1$, the pressure-fluctuation spectrum is dominated by a term $\rho^2(U_1-U_c)^2\phi_{11}(\omega)$ and therefore varies as ω^2 for small ω. This agrees with theoretical results for the wall-pressure spectrum. The disagreement with measurements of the wall-pressure spectrum is attributed to the effect of extraneous sound on the latter, because an acoustic velocity fluctuation of intensity $\overline{u_1^2}$ implies a pressure fluctuation intensity $\rho^2a_0^2\overline{u_1^2}$ compared with only $\rho^2(U_1-U_c)^2\overline{u_1^2}$ for a hydrodynamic velocity fluctuation.

I am indebted to Dr J. T. Stuart for the direct solution of equation (1), to Mr D. H. Ferriss for helpful discussions and for writing the computer programs, and to Mr M. G. Terrell for assistance with the experiments.

The work described in this paper forms part of the research programme carried out by the Aerodynamics Division of the National Physical Laboratory for the Ministry of Aviation, and the paper is published by permission of the Director of the Laboratory.

Appendix

(i) *Special results of Phillips's theory for an axisymmetric field*

To convert the one-dimensional wave-number spectrum $\phi_{22}(k_1)$ into the axisymmetric wave-number magnitude spectrum $\Phi_{22}(k)$ we require the inverse of the relation

$$\phi_{22}(k_1) = \int_{-\infty}^{\infty} \Phi_{22}(k)\,dk_3 = 2\int_0^{\infty} \Phi_{22}(k)\,dk_3. \tag{1}$$

Substituting

$$k_1^2 = 1/x, \quad k_1^2+k_3^2 \equiv k^2 = 1/z, \quad g(x) = x^{-\frac{1}{2}}\phi_{22}(x^{-\frac{1}{2}})$$

and

$$f(z) = z^{-\frac{3}{2}}\Phi_{22}(z^{-\frac{1}{2}}),$$

the relation becomes

$$g(x) = \int_0^x \frac{f(z)}{(x-z)^{\frac{1}{2}}}\,dz. \tag{2}$$

This is a special case of the integral equation solved by Margenau & Murphy (1947). The solution is

$$f(z) = \frac{1}{\pi}\frac{d}{du}\int_0^u \frac{g(x)\,dx}{(u-x)^{\frac{1}{2}}} \tag{3}$$

under the restriction $g(0) = 0$ or $\operatorname{Lt}_{k_1\to\infty}[k_1\phi_{22}(k_1)] = 0$, which is certainly satisfied by actual spectra. Finally,

$$\Phi_{22}(k) = \frac{1}{\pi}\frac{d}{dk}\left[k\int_{\infty}^{k} \frac{\Phi_{22}(k_1)\,dk_1}{k_1(k_1^2-k^2)^{\frac{1}{2}}}\right]. \tag{4}$$

Equation (1) can be inverted indirectly by taking the Fourier transform of $\phi_{22}(k_1)$ to give the (axisymmetric) correlation as

$$R_{22}(r) = R_{22}(r_1) = \int \phi_{22}(k_1) \cos k_1 r_1 \, dr_1. \tag{5}$$

Then

$$\Phi_{22}(k) = \frac{1}{(2\pi)^2} \iint R_{22}(r) \cos k_1 r_1 \cos k_3 r_3 \, dr_1 \, dr_3$$

$$= \frac{1}{(2\pi)^2} \int_0^{2\pi} \int_0^{\infty} R_{22}(r) \, r \cos (kr \cos \theta) \, dr \, d\theta, \tag{6}$$

where θ is the angle between $\mathbf{k}$ and $\mathbf{r}$. Integrating once, we obtain

$$\Phi_{22}(k) = \frac{1}{2\pi} \int_0^{\infty} R_{22}(r) \, J_0(kr) \, r \, dr, \tag{7}$$

a Hankel transform of order zero. The spectral form, (4), is rather more convenient for discussion of asymptotic behaviour, but the transform is obviously better for numerical calculation and perhaps for some analytical work, bearing in mind the vast number of known integrals with Bessel functions as kernels.

Only the u_2 spectrum, $\Phi_{22}(k)$, is axisymmetric: $\Phi_{11}(\mathbf{k})$ and $\Phi_{33}(\mathbf{k})$ are not. Phillips gives:

$$\Phi_{11}(\mathbf{k}) = k_1^2 k^{-2} \theta(k) \, e^{-2kx_2}, \tag{8a}$$

$$\Phi_{22}(\mathbf{k}) = \Phi_{22}(k) = \theta(k) \, e^{-2kx_2} = \Phi_{11}(\mathbf{k}) + \Phi_{33}(\mathbf{k}), \tag{8b}$$

$$\Phi_{33}(\mathbf{k}) = k_3^2 k^{-2} \theta(k) \, e^{-2kx_2}, \tag{8c}$$

where $\theta(k)$ is the spectrum of u_{20}, the normal velocity fluctuation in the plane $x_2 = 0$. We note that

$$\phi_{11}(k_1) = \int \Phi_{11}(\mathbf{k}) dk_3 = k_1^2 \int k^{-2} \Phi_{22}(k) dk_3, \tag{9}$$

so that $\phi_{22}(k_1)$ and $\Phi_{22}(k)$ can be replaced by $k_1^{-2} \phi_{11}(k_1)$ and $k^{-2} \Phi_{22}(k)$ in equation (1) and its inverse, equations (4) and (7). $\Phi_{22}(k)$ can therefore be derived directly from $\phi_{11}(k_1)$. Given $\Phi_{22}(k)$, $R_{22}(r)$ can be obtained by taking the (inverse) Hankel transform, and $\phi_{22}(k_1)$ is the Fourier transform of $R_{22}(r) \equiv R_{22}(r_1)$. Finally

$$\phi_{33}(k_1) = \phi_{11}(k_3) = \phi_{22}(k_1) - \phi_{11}(k_1)$$

from equation (3). $\phi_{11}(k_3)$ or its Fourier transform $R_{11}(0, 0, r)$ are relevant to the discussion of the fluctuating pressure field, below.

Since $\Phi_{11}(\mathbf{k}) = \frac{1}{2}(1 + \cos 2\psi) \, \Phi_{22}(\mathbf{k})$, where ψ is the angle between k_1 and $\mathbf{k}$, these derivations and some of the following ones could be expressed more neatly by introducing Hankel transforms of order two, but it was not considered worth while to write a computer program for this transform.

(ii) *Asymptotic results*

Various asymptotic results and approximations can be obtained for the one-dimensional and two-dimensional spectra in terms of one another. As can be seen from Phillips's analysis, continuity and axisymmetry require

$$\theta(k) \sim \theta_2 k^2 + O(k^4)$$

for small k (that is, for $k\delta_1 \ll 1$). The behaviour of $\theta(k)$ near $k = 0$ thus entirely determines the behaviour of $\Phi_{22}(k) = \theta(k)e^{-2kx_2}$ for large x_2/δ_1. It can be seen from figures 3 and 5 that the range of validity of the approximation $\theta(k) = \theta_2 k^2$ extends only as far as the peak of the $\phi_{11}(k_1)$ spectrum even at the largest value of x_2/δ_1, so that the asymptotic results for the spectra at large $k_1 x_2$ cannot yet be compared directly with experiment, but they are derived below for the sake of completeness.

If we take

$$\theta(k) = \sum_{n=2}^{\infty} \theta_n k^n$$

near $k = 0$ then $\phi_{11}(k_1)$ and $\phi_{22}(k_1)$ can be obtained as the sum of integrals like

$$\phi_n = \theta_n \int_{-\infty}^{\infty} k^n e^{-2kx_2} dk_3:$$

putting $k = k_1 \cosh u$, $k_3 = k_1 \sinh u$, $2k_1 x_2 = x$, we have

$$\int_{-\infty}^{\infty} k^n e^{-2kx_2} dk_3 = 2k_1^{n+1}(-1)^{n+1} \frac{\partial^{n+1}}{\partial x^{n+1}} \int_0^{\infty} e^{-x\cosh u}\, du$$

$$= 2k_1^{n+1}(-1)^{n+1} \frac{\partial^{n+1}}{\partial x^{n+1}} K_0(x) \equiv 2k_1^{n+1} K d_{n+1}(x), \quad \text{say,} \qquad (10)$$

where $K_0(x)$ is the modified Bessel function of the second kind of order zero ($\frac{1}{2}\pi K h_0(x)$ in the notation of Jeffreys & Jeffreys (1956)). This solution is analogous to the function $Ki_n(x)$, the n-fold *integral* of $K_0(x)$, tabulated by Bickley & Nayler (1935).

For small x

$$K_0(x) \sim -\log \tfrac{1}{2}x, \quad Kd_n(x) \sim \frac{(n-1)!}{x^n}, \quad \phi_n \sim \frac{\theta_n n!}{2^n x_2^{n+1}}, \qquad (11a,b,c)$$

so that $\phi_{22}(k_1)$ tends to a finite value as $k_1 \to 0$, unlike $\phi_{11}(k_1)$, which tends to zero as k_1^2: this result is obtainable directly by putting $k = |k_3|$ in the integral for ϕ_n.

For large x

$$K_0 \sim (\pi/2x)^{\frac{1}{2}} e^{-x}, \quad Kd_n(x) \sim (\pi/2x)^{\frac{1}{2}} e^{-x}, \quad \text{also} \quad \phi_n \sim \theta_n (\pi/x_2)^{\frac{1}{2}} k_1^{n+\frac{1}{2}} e^{-2k_1 x_2}. \qquad (12a,b,c)$$

A plausible form for $\theta(k)$ for *all* k would be $\theta_2 k^2 e^{-2kb}$, giving

$$\phi_{22}(k_1) \sim \theta_2 \left(\frac{\pi}{x_2+b}\right)^{\frac{1}{2}} k^{\frac{5}{2}} e^{-2k_1(x_2+b)} \quad \text{for large } k_1 x_2 \qquad (13a)$$

and

$$\phi_{22}(k) \sim \frac{\theta_2}{2(x_2+b)^3} \quad \text{for small } k_1 x_2. \qquad (13b)$$

Thus the condition for the sufficiency of the quadratic approximation to $\theta(k)$ is simply $x_2 \gg b$, which is equivalent to $x_2 \gg \delta_1$, since δ_1 and b are alternative scales of the energy-containing eddies. When this condition is satisfied and $\theta(k) \sim \theta_2 k_1^2$,

$$\phi_{22}(k_1) \sim \theta_2 (\pi/x_2)^{\frac{1}{2}} k_1^{\frac{5}{2}} e^{-2k_1 x_2} \quad \text{for large } k_1 x_2 \qquad (14a)$$

$$\sim \theta_2/2x_2^3 \quad \text{for small } k_1 x_2. \qquad (14b)$$

$\phi_{22}(0)$ cannot be thought of as the intensity of the largest eddies, as it is simply

$$2\int_0^\infty \Phi_{22}(k_3)\,dk_3.$$

The result is consistent with

$$\overline{u_1^2} = \overline{2u_2^2} = 2\pi\int_0^\infty \Phi_{22}(k)\,k\,dk \sim \frac{3\pi\theta_2}{8x_2^4}.$$

Now
$$\phi_{11}(k_1) = \int \frac{k_1^2}{k^2}\,\Phi_{22}(k)\,dk_3,$$

$$= 2\theta_2 k_1^3 K d_1(x) \quad \text{if} \quad \theta(k) \sim \theta_2 k^2,$$

$$\sim \theta_2\left(\frac{\pi}{x_2}\right)^{\frac{1}{2}} k_1^{\frac{5}{2}}\, e^{-2k_1x_2} = \phi_{22}(k_1) \quad \text{for large } k_1x_2, \tag{15a}$$

$$\sim \frac{\theta_2}{x_2}\,k_1^2 \text{ for small } k_1x_2. \tag{15b}$$

$\phi_{11}(k_1)$ and $\phi_{22}(k_1)$ are equal for large k_1x_2 because, for large k_1, $k = k_1$ throughout the range of k_3 which contributes to the integral for $\phi_{11}(k_1)$.

Putting $k = k_1\cosh u$, etc., we have

$$\Phi_{33}(k_1) = \int \frac{k_3^2}{k^2}\,\Phi_{22}(k)\,dk_3,$$

$$= \int \theta_2 k_1^3(\cosh^2 u - 1)\cosh u\, e^{-2k_1x_2\cosh u}\,du,$$

which contains a factor $Kd_3(x) - Kd_1(x)$ and is therefore of a smaller order of magnitude than $\phi_{11}(k_1)$ and $\phi_{22}(k_1)$ at large k_1x_2, since $\cosh^2 u \simeq 1$ unless $e^{-2k_1x_2\cosh u} \simeq 0$, by definition of 'large' k_1x_2. This is the result of the k_3^2/k^2 weighting factor which concentrates the power near the k_3-axis in the wave-number plane. The $\phi_{11}(k_3)$ spectrum behaves analogously. For small k_1x_2,

$$\phi_{33}(k_1) \sim \phi_{22}(k_1) - \phi_{11}(k_1)$$

as expected.

REFERENCES

Batchelor, G. K. 1956 *The Theory of Homogeneous Turbulence.* Cambridge University Press.

Bickley, W. G. & Nayler, J. 1935 *Phil. Mag.* (7), **20**, 343.

Bradbury, L. J. S. 1963 Ph.D. Thesis, Queen Mary College, University of London.

Bradbury, L. J. S. 1965 *J. Fluid Mech.* **23**, 31.

Bradshaw, P. 1965 *Nat. Phys. Lab. Aero. Rep.* no. 1172.

Bradshaw, P. 1966 *Nat. Phys. Lab. Aero. Rep.* no. 1184.

Bradshaw, P., Ferriss, D. H. & Johnson, R. F. 1964 *J. Fluid Mech.* **19**, 591.

Bradshaw, P. & Hellens, G. H. 1964 *Nat. Phys. Lab. Aero. Rep.* no. 1119.

Corcos, G. M. 1964 *J. Fluid Mech.* **18**, 353.

Dumas, R. 1964 *Pub. Sci. et Tech. du Min. de l'Air (Paris)*, no. 404.

Favre, A., Gaviglio, J. J. & Dumas, R. 1957 *J. Fluid Mech.* **2**, 313.

Ferriss, D. H. 1963 *Aero. Res. Counc. (Lond.) Curr. Pap.* no. 719.

Ffowcs Williams, J. E. 1960 *Southampton Univ., Dept. Aeron. and Astron. Rep.* no. 109.

Grant, H. L. 1958 *J. Fluid Mech.* **4**, 149.

HODGSON, T. H. 1962 *College of Aeronautics (Cranfield) Note*, no. 129.

JEFFREYS, H. & JEFFREYS, B. S. 1956 *Methods of Mathematical Physics*. Cambridge University Press.

KLEBANOFF, P. S. 1955 *Nat. Adv. Comm. Aero. (Wash.) Rep.* no. 1247.

LIEPMANN, H. W. 1954 *GALCIT/NACA Contract Rep.* NAW-6288 (*Aero. Res. Counc. (Lond.)*, no. 23515 (1962)).

LIEPMANN, H. W. 1962 *Mécanique de la turbulence, Marseilles*, 1961, Colloques Internat. du C.N.R.S. (Paris).

LILLEY, G. M. 1963 *College of Aeronautics (Cranfield) Note*, no. 140.

LILLEY, G. M. & HODGSON, T. H. 1960 *AGARD (Paris) Rep.* no. 276.

MARGENAU, H. & MURPHY, G. M. 1947 *The Mathematics of Physics and Chemistry*, p. 507. New York: Van Nostrand.

PHILLIPS, O. M. 1955 *Proc. Camb. Phil. Soc.* **51**, 220.

SERAFINI, J. S. 1963 *Nat. Aero. & Space Admin. (Wash.) Tech. Rep.* R-82.

STEWART, R. W. 1956 *J. Fluid Mech.* **1**, 593.

WILLS, J. A. B. 1964 *Nat. Phys. Lab. Aero. Rep.* no. 1131.

WILLS, J. A. B. 1965 Private communication.

WOOLDRIDGE, C. E. & WILLMARTH, W. W. 1962 Univ. of Michigan, *ORA Rep.* no. 02920.